Neutronics Performance of Axially-shielded Burnable Absorber (ABA) in the Equilibrium Cycle of Soluble Boron-Free SMR

Yunseok Jeong [a], Jaehyun Ryu [a], and Yonghee Kim [a*]
[a]*Nuclear and Quantum Engineering, KAIST*
[*]*Corresponding author: yongheekim@kaist.ac.kr*

Keywords : Axially-shielded burnable absorber, soluble boron-free, SMR

1. Introduction

Soluble boron-free (SBF) SMRs have attracted increasing interest because they can simplify the reactor system, improve inherent safety, and enhance load-follow capability. However, the elimination of soluble boron also makes core design much more challenging, since the large excess reactivity must be controlled almost entirely by burnable absorbers. Therefore, the successful deployment of SBF SMRs strongly depends on the development of a practical and effective burnable absorber design.

Conventional burnable absorbers have important limitations in this respect. Integral gadolinia burnable absorbers (IGD), although technologically mature and commercially proven, tend to suffer from rapid gadolinium depletion and consequent reactivity upswing under SBF conditions. They can also increase pin power peaking within a fuel assembly. Other commercial options, such as IFBA, Pyrex, and WABA, are also not ideal for SBF SMRs because they may reduce fuel inventory, increase linear heat generation, or interfere with control rod utilization.

Several new burnable absorber concepts have been proposed to overcome these limitations [1-3]. Although such concepts have shown promising neutronic performance, many of them still require new fabrication methods or face licensing and practical deployment challenges. For SBF SMRs, a desirable burnable absorber should not only provide effective cycle-long reactivity control, but also rely on a licensable and practically achievable design.

To address this need, the axially-shielded burnable absorber (ABA) was proposed as a practical burnable absorber concept based on conventional IGD technology [4]. By loading burnable absorber pellets only at selected axial locations, ABA aims to utilize axial self-shielding to control absorber depletion, while reducing fuel inventory penalty and minimizing pin power peaking. In this study, the neutronic performance of ABA is investigated for the equilibrium cycle of a soluble boron-free SMR, with emphasis on reactivity control, power distribution, and cycle performance.

2. Methods

2.1 Core Model

The present study considered a soluble boron-free SMR core whose basic specifications were referenced from the iSMR design [3]. Whole-core depletion calculations were performed to evaluate the neutronics performance of ABA in the equilibrium cycle. The main evaluation parameters include cycle reactivity behavior, radial and axial power distributions, fuel discharge burnup, and cold zero power shutdown margin.

2.2 ABA Design Concept

The axially-shielded burnable absorber (ABA) was proposed as a practical three-dimensional BA concept for SBF SMRs. Rather than uniformly distributing absorber material, ABA forms axially localized IGD regions by loading consecutive IGD pellets within each fuel rod. In this way, absorber depletion can be controlled through axial self-shielding by adjusting the number of consecutive IGD pellets and the gadolinia weight fraction.

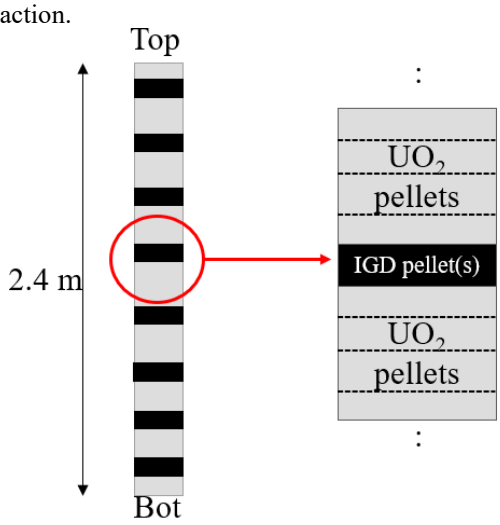

Figure 1 Concept of ABA fuel rod

To realize controlled depletion over the cycle, the ABA regions are classified into primary, secondary, and tertiary BA zones, as shown in Figure 2. The primary, secondary, and tertiary BA zones were designed with different gadolinia weight fractions so that the depletion completion timing of each region could be controlled over the cycle. Accordingly, the primary BA remains effective until near EOC, the secondary BA mainly suppresses early- and mid-cycle excess reactivity, and the tertiary BA is placed near the top and bottom of the

fuel column to suppress initial excess reactivity and mitigate axial power skewness. The U-235 enrichment in the ABA regions was adjusted according to Eq. (1), while the TBA regions located at both axial ends employed 2.85 wt% U-235 to mitigate axial power skewness.

$$4.65 \times (1 - 0.05 \times wt\%) \quad (1)$$

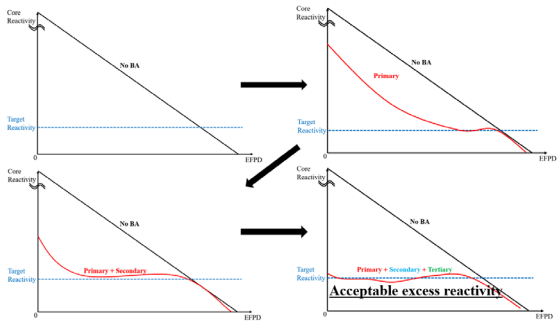

Figure 2 Reactivity control via ABA

2.3 ABA Modeling for the Equilibrium Cycle

In the equilibrium cycle, all fresh fuel assemblies were assumed to employ 4.95 wt% U-235 enrichment. Since fresh fuel of this enrichment is repeatedly introduced, a larger BA inventory is required than in the initial cycle.

As shown in Figure 3, two ABA assembly types were employed in the equilibrium core. 0.12 wt% erbia was additionally doped into the normal UO_2 fuel of Zone 1 in order to provide finer reactivity control. Basically, 2 cm-thick IGD pellets were used for the ABA regions. However, in Zone 1, which is mainly loaded near the core center, a lower initial reactivity was required, and thus the primary BA regions employed 3 cm-thick IGD pellets.

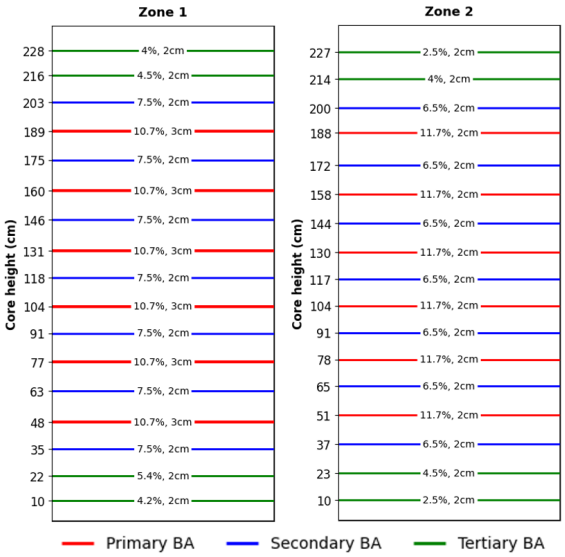

Figure 3 Axial configuration of ABA fuel assemblies in the equilibrium cycle

2.4 Fuel Shuffling Scheme

A multi-batch fuel management scheme was adopted to establish the equilibrium cycle, as shown in Figure 4. In each cycle, 35 out of 69 fuel assemblies were reloaded, while the others were shuffled according to a predetermined radial loading pattern. The central assembly was burned and discharged every cycle, and the same assembly design as that used at the core center in the initial cycle was adopted for this position.

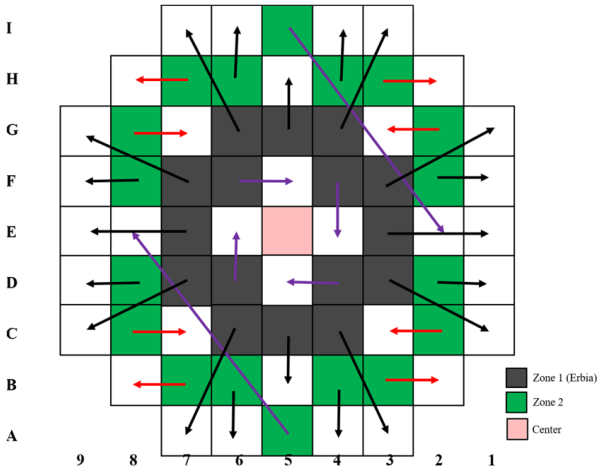

Figure 4 Fuel shuffling scheme

2.5 Control Rod Material and Pattern

Different control rod materials were assigned according to the function of each bank. The gray banks employed hafnium rods coated with 5 mm of Inconel 625 for cycle reactivity control. The regulating banks used natural B_4C, while the shutdown banks used 95 wt% enriched B_4C to ensure shutdown margin.

Figure 5 shows the control rod pattern adopted in this study. Based on this configuration, the cold zero power shutdown margin of the ABA-loaded equilibrium core was evaluated.

Table 1 Rod material

Bank	Material
MS1, MS2	Inconel cladded Hf
R3, R2, R1	Natural B_4C
SB	95 wt% enriched B_4C

	5	4	3	2	1
E	MS2	SB	R3	SB	SB
D	SB	MS1		R1	SB
C	R3		R2	SB	
B	SB	R1	SB	SB	
A	SB	SB			

Figure 5 Control rod pattern

3. Numerical Results

For the numerical results presented in this section, whole-core depletion calculations were performed using SERPENT 2 with 300,000 particles, 100 inactive cycles, and 200 active cycles under equilibrium xenon conditions [5]. The fuel temperature was fixed at 903.15 K, while the coolant temperature was linearly interpolated along the axial direction to match the inlet and outlet temperatures.

3.1 Reactivity Curve

Figure 6 shows the cycle reactivity curves of the ABA-loaded equilibrium core from cycle 4 to cycle 7. As the fuel shuffling process was repeated, the cycle-wise reactivity behavior converged to a nearly repetitive pattern. In particular, cycles 6 and 7 showed very similar reactivity curves, indicating that the equilibrium cycle was practically established. The core exhibited a reactivity upswing of about 1700 pcm during the cycle, and the cycle length was 800 EFPD. The standard deviation of the reactivity curve is 12 pcm.

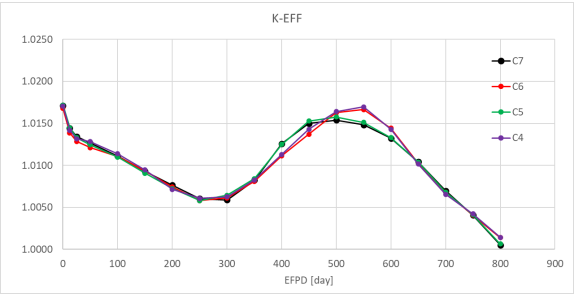

Figure 6 Reactivity curve (Cycles 4-7)

3.2 Power Distribution in the Equilibrium Cycle

The radial and axial power distributions of cycles 6 and 7 were compared at BOC, 300 EFPD, and 800 EFPD. The axial power distributions are shown in Figures 7, 9, and 11, while the corresponding radial power distributions are shown in Figures 8, 10, and 12. The relative standard deviations of axial power profile and radial power profile are 0.25% and 0.22% respectively.

Overall, the radial power distributions of cycles 6 and 7 were very similar, confirming that the equilibrium state was practically established. The three-dimensional assembly-wise peaking factors were 2.12/2.14 at BOC, 1.94/1.97 at 300 EFPD, and 1.93/1.95 at 800 EFPD for cycles 6 and 7.

In the axial power distributions, the upper and lower skewness of cycles 6 and 7 appear to alternate. This is attributed to slight axial differences in gadolinia depletion within the ABA regions, which cause small changes in the axial reactivity distribution from cycle to cycle. Nevertheless, the overall power distribution remained acceptable throughout the equilibrium cycle.

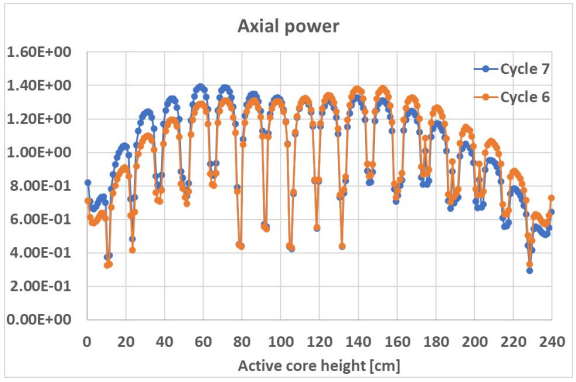

Figure 7 Axial power distribution at BOC

	9	8	7	6	5	4	3	2	1
I			0.532	0.701	0.777	0.692	0.517		
H		0.679	1.012	1.118	1.050	1.102	0.980	0.660	
G	0.562	1.048	1.211	1.194	1.185	1.182	1.180	1.022	0.550
F	0.769	1.226	1.242	1.253	1.261	1.252	1.227	1.205	0.760
E	0.799	1.309	1.274	1.282	1.211	1.278	1.260	1.293	0.791
D	0.760	1.216	1.245	1.268	1.277	1.262	1.235	1.203	0.755
C	0.552	1.037	1.204	1.202	1.204	1.197	1.205	1.030	0.551
B		0.673	1.008	1.128	1.071	1.128	1.005	0.667	
A			0.534	0.708	0.794	0.707	0.529		

Figure 8 Radial power distribution at BOC

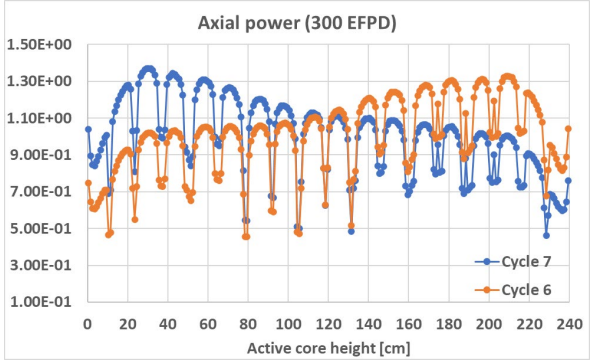

Figure 9 Axial power distribution at 300 EFPD

	9	8	7	6	5	4	3	2	1
I			0.520	0.688	0.776	0.687	0.526		
H		0.673	1.020	1.139	1.008	1.142	1.024	0.674	
G	0.532	1.045	1.177	1.241	1.228	1.247	1.189	1.054	0.536
F	0.711	1.233	1.296	1.285	1.160	1.288	1.305	1.235	0.716
E	0.724	1.261	1.320	1.172	1.163	1.178	1.333	1.262	0.726
D	0.712	1.237	1.304	1.282	1.158	1.292	1.311	1.238	0.715
C	0.531	1.050	1.187	1.245	1.231	1.255	1.196	1.054	0.534
B		0.681	1.028	1.147	1.017	1.153	1.033	0.682	
A			0.526	0.697	0.787	0.694	0.529		

Figure 10 Radial power distribution at 300 EFPD

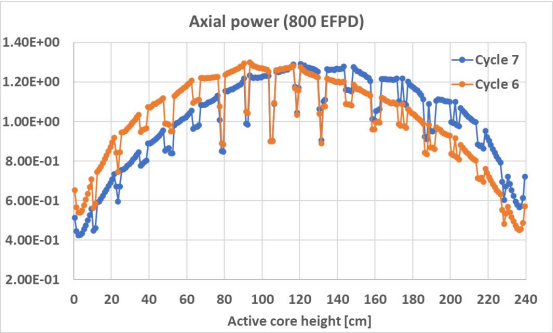

Figure 11 Axial power distribution at 800 EFPD

	9	8	7	6	5	4	3	2	1
I			0.496	0.661	0.848	0.660	0.497		
H		0.615	1.061	1.238	1.000	1.240	1.064	0.617	
G	0.461	1.032	1.091	1.434	1.443	1.444	1.094	1.031	0.461
F	0.574	1.188	1.426	1.429	1.080	1.423	1.423	1.183	0.571
E	0.555	1.039	1.431	1.077	1.062	1.075	1.428	1.044	0.559
D	0.579	1.197	1.433	1.437	1.087	1.437	1.438	1.207	0.582
C	0.465	1.044	1.104	1.451	1.448	1.451	1.103	1.045	0.468
B		0.619	1.063	1.232	0.995	1.237	1.063	0.620	
A			0.495	0.654	0.842	0.656	0.494		

Figure 12 Radial power distribution at 800 EFPD

3.3 Fuel Discharge Burnup

Figure 13 shows the assembly-wise discharge burnup distribution of the equilibrium core. The average discharge burnup was 40.2 GWd/tU including the center fuel assembly and 40.7 GWd/tU excluding it.

		37.50	36.20		36.10	37.30			
	33.00			47.80			32.90		
38.30		44.40				44.30		38.30	
37.40				54.30				37.30	
42.30	39.80		54.60	23.50	54.60		39.80	42.30	
37.30				54.40				37.40	
38.10		44.30				44.20		38.30	
	33.00			47.80			32.90		
		37.40	36.20		36.10	37.40			

Figure 13 Fuel discharge burnup

3.4 Cold Zero Power (CZP) Shutdown Margin

The cold zero power shutdown margin was evaluated at 298 K by calculating k_{eff} for the all-rods-in condition and the N-1 condition with the D5 control rod assembly stuck with 2,000,000 particles. In both cases, sufficiently low and conservative k_{eff} values were obtained, confirming adequate shutdown capability.

Condition	k_{eff}
BOC	0.877464 ± 6.7 pcm
MOC	0.858195 ± 7.0 pcm
EOC	0.870834 ± 7.3 pcm
BOC (N-1)	0.902073 ± 6.4 pcm
MOC (N-1)	0.876641 ± 6.9 pcm
EOC (N-1)	0.881453 ± 7.4 pcm

4. Conclusions

The neutronics performance of the axially-shielded burnable absorber (ABA) was investigated for the equilibrium cycle of a soluble boron-free SMR based on the iSMR core specification. ABA was applied as a practical burnable absorber concept using localized IGD regions, and additional 0.12 wt% erbia doping was introduced to achieve finer initial reactivity control.

The whole-core depletion results showed that the equilibrium cycle was practically established, with cycles 6 and 7 exhibiting nearly repetitive reactivity behavior. The core showed a reactivity upswing of about 1700 pcm and a cycle length of 800 EFPD. The radial and axial power distributions remained acceptable throughout the cycle, and the slight cycle-to-cycle change in axial power shape was attributed to axial differences in gadolinia depletion. The average discharge burnup was 40.2 GWd/tU including the center assembly and 40.7 GWd/tU excluding it. The cold zero power shutdown margin at 298 K also showed sufficiently low and conservative k_{eff} values for both all-rods-in and N-1 stuck rod conditions.

Overall, the results demonstrate that ABA is a practical and effective burnable absorber concept for equilibrium-cycle operation of soluble boron-free SMRs.

REFERENCES

1. X. H. Nguyen, C. H. Kim, and Y. H. Kim, “An advanced core design for a soluble-boron-free small modular reactor ATOM with centrally-shielded burnable absorber,” Nuclear Engineering and Technology, vol. 51, no. 2, pp. 369–376, Feb. 2019, doi: 10.1016/j.net.2018.11.016.
2. S. Wijaya, X. H. Nguyen, Y. Jeong, and Y. H. Kim, “Multi-batch core design study for innovative small modular reactor based on centrally-shielded burnable absorber,” Nuclear Engineering and

Technology, vol. 56, no. 3, pp. 907–915, Mar. 2024, doi: 10.1016/j.net.2023.11.007.

3. J. S. Kim, et al., "Highly Intensive Gadolinium/Alumina (HIGA) burnable absorber rods for soluble-boron-free i-SMR core," in Proc. Korean Nuclear Society Spring Meeting, 2024.
4. Y. Jeong, J. Ryu, D. Choi, Y. Lee, and Y. Kim, "Axially-shielded Burnable Absorber (ABA) for Soluble Boron-Free SMR: Neutronics Feasibility in the Initial Cycle," *Transactions of the Korean Nuclear Society Autumn Meeting*, October 30-31, 2025.
5. J. Leppänen, M. Pusa, T. Viitanen, V. Valtavirta, and T. Kaltiaisenaho, "The Serpent Monte Carlo code: Status, development and applications in 2013," Annals of Nuclear Energy, vol. 82, pp. 142–150, Aug. 2015, doi: 10.1016/j.anucene.2014.08.024.